RETRIEVAL OF SURFACE LAMBERT ALBEDOS AND AEROSOLS OPTICAL DEPTHS USING OMEGA NEAR-IR EPF OBSERVATIONS OF MARS. M. Vincendon, Y. Langevin[1], F. Poulet[1], J.P. Bibring[1], B. Gondet[1] and the OMEGA team. [1]Institut d'Astrophysique Spatiale, CNRS/Université Paris 11, Orsay, France, mathieu.vincendon@ias.fr.

Introduction:
The visible and near-IR imaging spectrometer OMEGA has acquired around ten emission phase function (EPF, or "spot pointing") sequences up to now over different kinds of surfaces: bright and dark ice-free surfaces, H_2O and CO_2 ice covered surfaces. EPF sequences are ideally suited for the derivation of aerosols properties and such studies have been carried through with the broad band channel centred on 0.67µm of IRTM [1], and then TES [2]. EPF sequences are also appropriate for the retrieval of surface reflectance spectra free of aerosols contribution, as will be done with CRISM/MRO [3, 4]. We have performed the analysis of 5 spot pointing observations acquired by OMEGA in the near-IR (0.95-2.65µm corresponding to the C-channel). These EPF sequences present large variations of the emergence angle but moderate variations of the phase angle. The reflectance factor (defined by I/F/cos(i)) strongly varies during these sequences, whereas it would have been constant for a lambertian surface and no aerosols. Observations of a wide range of surface material by the Mars Exploration Rovers [5] have shown that the differences between the observed photometric functions and the Lambert model at moderate phase angles are low. We have approximated the Martian surface with a Lambert model and we have analyzed the OMEGA EPF sequences in terms of aerosols contribution to retrieve simultaneously the optical depth of aerosols and the Lambert albedo of the surface.

Aerosols model:
A look-up table of reflectance factors is populated by the Monte-Carlo based model of [6] as a function of Lambert albedo of the surface, optical depth of aerosols, and geometry of observation (defined by the solar incidence angle, the emergence angle and the azimuth angle). This model takes into account multiple scattering by aerosols and multiple interactions between the surface and the aerosols. The layer of aerosols is modeled by three parameters: the optical depth, the particle phase function and the single scattering albedo. We have selected a single-lobed Henyey-Greenstein (HG) phase function with an asymmetry parameter g=0.63 and a single scattering albedo of 0.974 between 1 and 2.6µm according to [6, 7]. Each spot pointing observation is then fitted by adjusting only 2 parameters at each wavelength: the optical depth of aerosols $\tau(\lambda)$ and the Lambert albedo of the surface $A_L(\lambda)$.

Observations:
The IFOV of OMEGA is constant during a spot pointing observation. As the distance varies, the pixel size varies by up to a factor 10 for high emergence (85°). The pixel size is typically of 1 to 4km in the nadir configuration depending on the position of the satellite on its elliptical orbit. The pointing accuracy during EPF observations reaches a precision of a few kilometers for the last sequences.

▪ **Orbit n°2610:** This orbit is centered on the Opportunity landing site (2°S, 354°E) at L_S 0.93° (23/01/2006). The large observed variations of the reflectance factor at 1µm from ~0.34 to 0.20 can be modeled with a Lambert surface albedo of 0.17 ± 0.01 and an optical depth of aerosols of 0.56 ± 0.10 (see Figure 1).

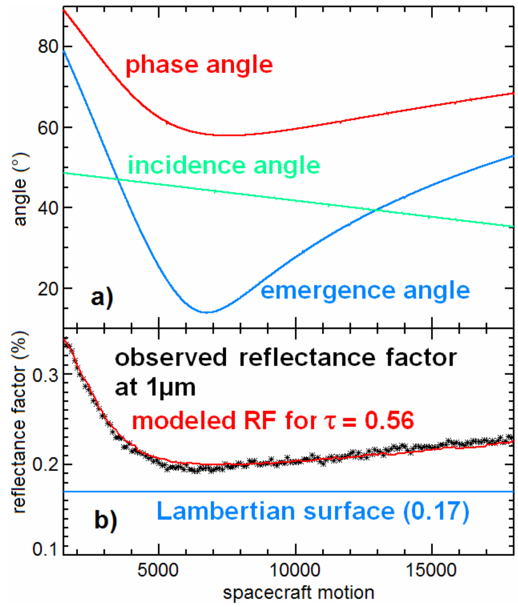

Figure 1: Orbit 2610 over the Meridiani landing site. a) variation of the geometry of observation during the sequence. b) variation of the reflectance factor (black) and fit of this variation (red) by a Lambert surface (blue) with an optical depth of aerosols of 0.56. See text for details.

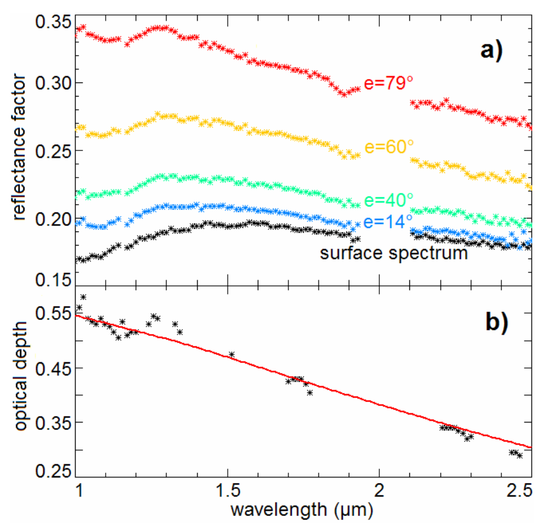

Figure 2: a) observed near-IR spectra during the EPF sequence of orbit n°2610 for different emergences (colors) and modeled spectrum of the surface (black). b) retrieved spectrum of the optical depth (black crosses, corresponding to spectral regions without atmospheric absorptions by gaz). The model derived with the method of [6] is indicated in red.

The value obtained at 1µm (0.56 ± 0.10) is similar to that derived by Pancam/Opportunity at 0.88µm during this period (0.656, 0.674, 0.687 [8]) considering the variations of the observed surface during the sequence (40km: the sequence cover surfaces with different albedos). The spectrum of surface Lambert albedos and the spectral variations of the optical depth between 1µm and 2.5µm are shown in Figure 2.

▪ **Orbit n°2772:** The spot pointing observation of orbit n°2772 (L_S 22.8, 9 March 2006) is centered on 25°S, 275°E, with a small drift of 9km of the targeted region. The region is homogeneous and we can reasonably consider that we observe the same surface albedo during the whole sequence. The model provides a satisfactory fit of the reflectance factor sequence with a Lambert surface reflectance and a low optical depth of aerosols (0.2 at 1µm) for all wavelengths in the 0.95 – 2.65 µm range (see Figure 3).

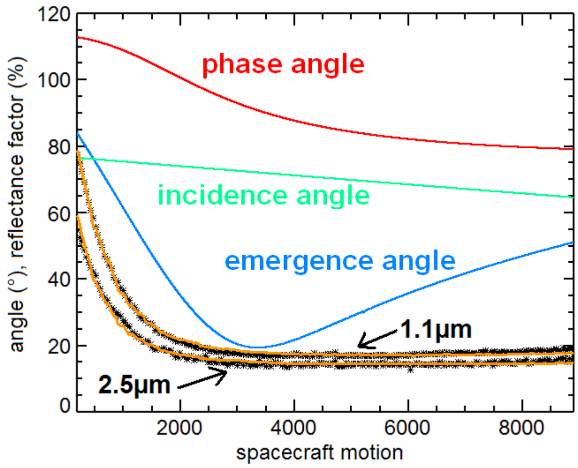

Figure 3 : Orbit n°2772 centred at 25°S, 275°E (L_S 23°). The observed variations of the reflectance factor are indicated in black for 2 wavelengths (1.1µm, top and 2.5µm, bottom). The model provides a good fit of the sequence (yellow lines) with τ=0.2 and A_L=0.133 for 1.1µm and with τ=0.113 and A_L=0.124 for 2.5µm.

▪ **Orbit n°3049:** A region covered by water ice (232.5°E, 74.75°N) at L_S 57.7° (26 May 2006) as been observed during orbit n°3049. The variations of the reflectance factor during the sequence are also almost fully understood by aerosols for both low reflectance regions of the spectrum (absorption bands) and bright continuum (Figure 4). Variations of the pointed region are < 3km before 5500 (abscissa in Figure 4), but the pointing drift between 5500 and 6500 (20 km). This can explain the difference between the best model fit and the observation for 1.39µm (continuum). Another possible reason can be photometric effects of the surface ice in the continuum.

▪ **Orbits n°2668 & 2139:** A good fit has also been obtained with the spot pointing sequence acquired over Hellas (orbit n°2668) and the south CO_2 cap (orbit n°2139, see [9]). The results of the model are similar with a Lambert hypothesis for the surface and the selected properties of dust aerosols.

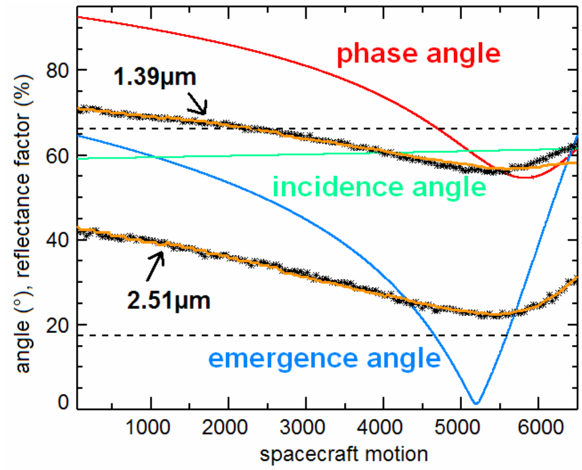

Figure 4 : Orbit n°3049 above water ice. The observed variations of the reflectance factor are indicated in black for two wavelengths (1.39µm, corresponding to the continuum of the ice spectrum, and 2.51µm in an absorption band). A satisfactory model fit (yellow lines) is obtained with τ=0.975 and A_L=0.663 for 1.39µm and with τ=0.80 and A_L=0.174 for 2.51µm (the Lambert albedo are indicated as dotted lines).

Conclusions:

▪ The aerosol contribution dominates the variations of the reflectance factor during EPF sequences observed by OMEGA between 0.95µm and 2.65µm. The Lambert hypothesis for the different surface types analyzed here (dark and bright ice-free surfaces, H_2O and CO_2 ice surfaces) provides satisfactory fits with moderate phase angles and large emergence angle variations.

▪ The aerosol scattering properties selected for this study on the basis of previous work [6, 7] (a constant HG phase function with g=0.63 and a constant single scattering albedo of 0.974) are adequate to reproduce the behavior of aerosols over large variations of the geometry of observations between 0.95µm and 2.65µm.

▪ This analysis is performed using an automatic routine (inputs: the observed reflectance factor and the geometry of observation; outputs: the optical depth τ and the Lambert albedo of the surface A_L for each wavelength between 0.95µm and 2.65µm) which minimizes the quadratic spread between the observed reflectance factor variations and the predicted variations for different couple of (τ, A_L). This approach can be used to evaluate the impact of aerosols on other datasets (e.g. CRISM). The surface reflectance spectra and the local optical depth of aerosols can then be retrieved.

References:

[1] Clancy R. T. and S. W. Lee, *Icarus*, **93**, 135 (1991). [2] Clancy R. T. et al., *J. Geophys. Res.,* **108**(E9), 5098 (2003). [3] McGuire P. C. et al., *Lunar Plant. Sci.* **37**, 1529 (2006). [4] Wolff M. J. et al., *AGU*, **P23B0060** (2006). [5] Johnson, J. R. et al., *J. Geophys. Res.*, **111**(E2), E02S14 (2006) [6] Vincendon M. et al., *J. Geophys. Res.,* accepted (2007). [7] Ockert-Bell M. E. et al., *J. Geophys. Res.* **102**, 9039 (1997). [8] Lemmon M. T. et al., *Science*, 306, 1753 (2004). [9] Vincendon M. et al., *LPSCXXXVIII*, this conference.